Available online at www.sciencedirect.com
ScienceDirect
Applied Catalysis B: Environmental 79 (2008) 356–367
APPLIED CATALYSIS B: ENVIRONMENTAL
www.elsevier.com/locate/apcatb

Oxygen partial pressure-dependent behavior of various catalysts for the total oxidation of VOCs using cycled system of adsorption and oxygen plasma

Hyun-Ha Kim *, Atsushi Ogata, Shigeru Futamura

National Institute of Advanced Industrial Science and Technology (AIST), AIST Tsukuba West, 16-1 Onogawa, Tsukuba, Ibaraki 305-8569, Japan

Received 11 December 2006; received in revised form 30 October 2007; accepted 31 October 2007

Abstract

In this work, comprehensive investigation was done on the oxygen partial pressure-dependent behavior of the various catalysts using a flow-type plasma-driven catalyst (PDC) reactor. These data provide a useful guideline for the optimization of the cycled system using adsorption and the O_2 plasma-driven catalysis of adsorbed volatile organic compounds (VOCs). The potentials of the tested catalysts for the cycled system were evaluated based on the enhancement factor and the adsorption capability. All the tested materials (TiO_2, γ-Al_2O_3, zeolites) exhibited positive enhancement factor, while negative values with the dielectric-barrier discharge (DBD) plasma alone. TiO_2 catalysts showed the highest enhancement factor of about 100 regardless of the type of metal catalysts and their supporting amount. Based on the experimental findings in this study and the literature information, a plausible mechanism of plasma-driven catalysis of VOCs was suggested.

Keywords: Nonthermal plasma; Oxygen plasma; VOCs; Total oxidation; Catalyst; Enhancement factor

1. Introduction

Volatile organic compounds (VOCs) released into the atmosphere as a consequence of man-made emission undergo a complex physical–chemical transformations before they are decomposed or deposited to the earth's surface. VOCs are directly related to the formation of photochemical smog and secondary aerosol in urban areas. Many of these VOCs are considered to be carcinogenic, teratogenic and mutagenic. Source reduction and process modification alone cannot meet the regulation in many cases. There is, therefore, an urgent need to develop more effective and inexpensive techniques for the treatment of VOCs.

There have been extensive researches on using nonthermal plasmas (NTPs) to remove various types of gas-phase hazardous pollutants over the last two decades [1–4]. One of the remarkable recent trends in air pollution control using NTP is the combination of NTP with catalysts in either of single-stage [5–7] or two-stage configuration [8–14]. The authors have been studied the decomposition of VOCs using single-stage plasma-driven catalyst (PDC) system [15–18]. Typical temperature window of the PDC system is below 373 K, where the normal thermal catalytic reactions do not occur. Low temperature operation is also advantageous to the lifetime of catalyst by preventing the agglomeration of metal catalyst due to thermal sintering. The PDC system is superior to the conventional NTP alone in terms of decomposition efficiency, CO_2 yield and good carbon balance (less aerosol formation). Since as the specific input energy (SIE) increases the formation of NO_x increases [16,19–21], operating range of SIE in the flow-type PDC system should be determined based on the trade-off between the removal efficiency and the NO_x formation. Therefore the flow-type PDC system can only be used for the treatment of dilute VOCs, which can be operated at relatively low SIE.

The authors first reported the strong O_2 partial pressure-dependent nature of the PDC system, packed with 2.0 wt% Ag/TiO_2 catalysts, for the decomposition of 200 ppm benzene [22]. Both the decomposition efficiency and the CO_2 selectivity were observed to increase remarkably with increasing O_2 partial

* Corresponding author.
E-mail address: hyun-ha.kim@aist.go.jp (H.-H. Kim).

0926-3373/$ – see front matter © 2007 Elsevier B.V. All rights reserved.
doi:10.1016/j.apcatb.2007.10.038

pressure in the gas stream. Based on this finding, the authors proposed the cycled system consisting of adsorption and the decomposition of adsorbed VOCs using O_2 plasma-driven catalysis (O_2-PDC). This cycled system is very promising technology in terms of complete oxidation of VOCs, high CO_2 selectivity, and suppression of nitrogen oxides formation. For the catalysts to be effective in the cycled system, they must have a positive O_2 partial pressure-dependence on both decomposition efficiency and the CO_2 selectivity.

In this work we focused on the O_2 partial pressure-dependent behavior of various catalysts for the further optimization of the cycled system. Three representative catalyst materials of TiO_2, γ-Al_2O_3 and zeolites were tested as well as the various metal catalysts. The potential of the tested materials for the cycled system was evaluated in terms of enhancement factor and adsorption capacity. We will also present a plausible mechanism responsible for the VOC destruction in the PDC system based on the experimental data in this study together with those in literature.

2. Experimental description

2.1. Plasma reactors and set-up

Fig. 1 shows the details of the PDC reactor and a dielectric-barrier discharge (DBD) reactor. The PDC reactor was basically similar to a cylindrical surface discharge reactor. A coil-type electrode with 35 turns and 0.45 mm diameter was set inside the tube as a high-voltage electrode, and silver paste was painted on the outside the quartz tube as a ground electrode. In this configuration, strong electrical field to form electrical discharge plasma is established between the ground electrode and the coil electrode on the inner surface of the quartz tube. Therefore, the dielectric constants of the packing materials have minor influence in generating plasma. The inner diameter and the effective length of the quartz tube were 13 mm and 200 mm, respectively. Catalysts in the PDC reactor were placed within the effective length of the reactor. This configuration rendered all the catalysts exposed to the plasma and also allowed to ignore additional adsorption or additional chemical reactions outside the plasma region. The amount of catalyst was about 25 cm^3.

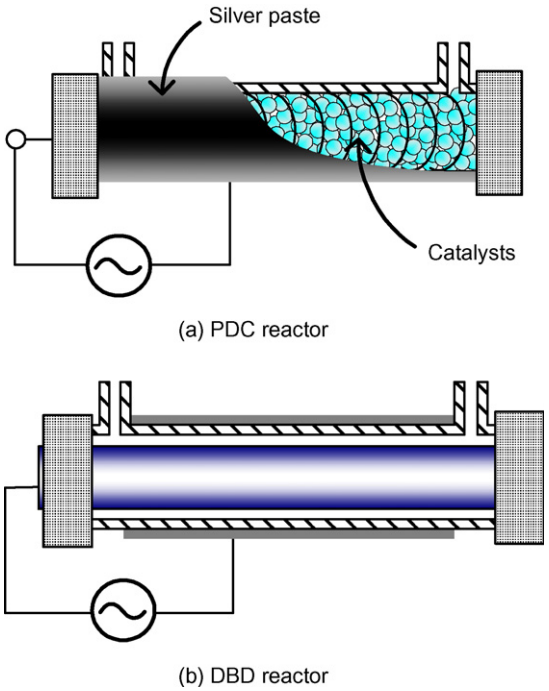

Fig. 1. Schematic diagram of plasma reactors: (a) plasma-driven catalyst (PDC) reactor and (b) dielectric-barrier discharge (DBD) reactor.

The DBD reactor was made of a Pyrex glass tube (33 mm inner diameter, 300 mm long) and stainless steel tube (30 mm diameter). The DBD reactor was cleaned up by oxygen plasma prior to each run to remove carbon deposition inside the reactor well. All the flow experiments were done at 373 K except for the thermal catalysis and the DBD reactor (room temperature). However, the actual temperature in the PDC reactor was slightly higher than 373 K due to the heating by the plasma. For the most of flow experiments, gas flow rates were set at 4–5 L min^{-1}, which corresponded to the gas hourly space velocity (GHSV) of 22,000–28,000 h^{-1}. The GHSV was calculated based on the gas residence time in the void of catalyst bed [16]. For the H-Y and molecular sieve-13X (MS-13X) having large adsorption capability, the flow rates were set at 10 L min^{-1} to accelerate the time to reach equilibrium state. The concentration of benzene or toluene was adjusted by changing either the temperature of water bath or the N_2 flow rate purging the bubbler. The concentration of VOCs was 200 ppm for the flow-type PDC experiment.

2.2. Cycled system

Since the general feature of the cycled system and the preliminary result of benzene decomposition have been already reported in a previous work [22], only brief description will be

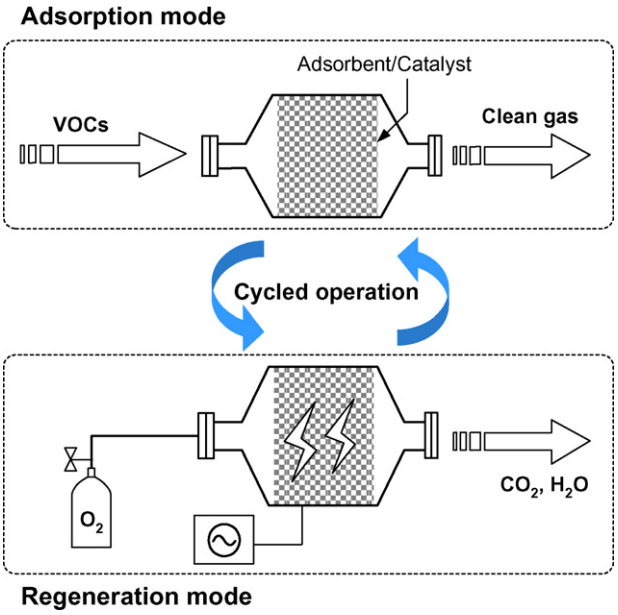

Fig. 2. Schematic diagram of the cycled system.

given here. Fig. 2 shows the schematic diagram of the cycled system. The cycled system is operated at room temperature, which is advantageous to adsorption. In the adsorption mode (plasma off), VOCs are removed by adsorption on the catalyst bed. When the catalyst bed reaches adsorption saturation, then VOCs containing gas stream are switched to another adsorption bed. The saturated catalyst bed is exposed to oxygen plasma to decompose the adsorbed VOCs. The O_2 plasma was turned on for 25–40 min depending on the conditions (mainly input power). Gas flow rates during the adsorption mode were set at 4–5 L min^{-1} unless other wise noted. Since the oxygen plasma does not produce any N_xO_y, it can be operated at high applied voltage and frequency. In this work, the regeneration mode was operated with oxygen flow in the range of 5–8 L min^{-1} for the measurement purpose. To decompose VOCs desorbed from catalyst just after the plasma was turned on, a small additional PDC reactor was connected during the regeneration mode [22]. In practical viewpoint, the regeneration mode can be operated in a closed system. After purging the catalyst bed with oxygen, the valves at both ends are closed before applying oxygen plasma.

2.3. Catalysts

Table 1 summarizes the characteristics of the catalysts used in this study. The tested catalysts can be divided into three groups of TiO_2, γ-Al_2O_3 and zeolites; TiO_2 (Sakai Chemical Co.), γ-Al_2O_3-A (Mizusawa Chemical Co.), γ-Al_2O_3-B (NE Chem. CAT Co.), MS-13X (Sigma–Aldrich Co.), ferrierite and H-Y (Tosoh Co.). TiO_2 pellet was anatase type, which is well known as a photocatalyst. All the metal catalysts except for gold (Au) were supported by impregnation method using their standard solutions. After several processes of drying and heating, the catalysts were calcined at 873 K for 10 h in air. The Au catalyst was supported on the TiO_2 pellets by deposition–precipitation method [23]. The size of Au catalyst was determined by a high-resolution transmission electron microscopy (TEM, Hitachi H-9000NAR). The diameter of the Au particles on the TiO_2 pellets was in range of 3–7 nm, which exhibits very high catalytic activity for CO oxidation even at 200 K [24,25]. The size of the other metal catalysts supported by impregnation ranged between 25 nm and 30 nm, except for the Pt (4–8 nm). Supporting of the metal catalysts on the TiO_2, γ-Al_2O_3 and zeolites slightly reduced the BET surface areas. For example, the BET area of fresh TiO_2 (68 m^2/g) was reduced to about 59 m^2/g by supporting 2.0 wt% of silver catalyst. Since the tested catalyst materials have different pellet size and specific weight, the amount of catalyst packed in the plasma reactor was set by volume (about 25 cm^3) rather than weight.

2.4. Electrical and optical measurements

The PDC reactor and the DBD reactor were energized by an AC high-voltage amplifier (Trek, 20/20B) and a function generator (Tektronix, AFG 310). The waveforms of the charge and the applied voltage were monitored with a digital oscilloscope (Tektronix, TDS3032B). The discharge waveforms of applied voltage and discharge current for the various catalysts have been reported elsewhere [18]. Discharge power was measured by the V-Q Lissajous program. SIE was calculated with the following relations for the flow-through

Table 1
Details of the catalysts

Catalyst	Loading metal	BET surface area (m^2/g)	Shape	Weight per volume (g/cm^3)	Size (mm)
TiO_2	Ag (~4 wt%)	≤ 68	spherical	1.01	1.8
TiO_2	Pt (1 wt%)	< 68	spherical	1.01	1.8
TiO_2	Ni (2 wt%)	< 68	spherical	1.01	1.8
TiO_2	Au (2 wt%)	< 68	spherical	1.01	1.8
γ-Al_2O_3-A	Ag (0, 0.5, 5 wt%)	≤ 210	spherical	0.61	2
γ-Al_2O_3-A	Ce (1, 5 wt%)	< 210	spherical	0.61	2
γ-Al_2O_3-B	Pt (0.5 wt%)	95	pellet	0.92	φ3.2×3.6
γ-Al_2O_3-B	Pd (0.5 wt%)	95	pellet	0.92	φ3.2×3.6
Ferrierite	-	270	extrusion	0.53	φ1.5×~5
MS-13X	-	540	extrusion	0.58	φ1.6×~4
H-Y	Ag (0, 2 wt%)	520	extrusion	0.53	φ1.5×~5

experiments.

$$\text{Specific input energy}\left(\frac{J}{L}\right) = \frac{P_{\text{dis}}}{Q_{\text{f}}} \times 60 \quad (1)$$

where the flow rate, Q_{f}, is in L min^{-1}. The term of $P_{\text{dis}}/Q_{\text{f}}$ is basically identical to the specific corona power, which was used in the field of electrostatic precipitator [26]. Both of SIE and specific corona power is the ratio of discharge power and gas flow rate. SIE value was varied by changing either applied voltage (~30 kV_{pk-pk} or frequency (100–800 Hz).

In the case of the cycled operation equivalent specific input energy (SIE_{eq}) was introduced to evaluate the energy consumption.

$$\text{SIE}_{\text{eq}}\left(\frac{J}{L}\right) = \frac{(P_{\text{dis}})_{\text{Ave}}}{(Q_{\text{Ads}})_{\text{f}}} \times \frac{t_{\text{Oxy}}}{t_{\text{Ads}}} \times 60 \quad (2)$$

Here, $(P_{\text{dis}})_{\text{Ave}}$ and $(Q_{\text{Ads}})_{\text{f}}$ indicate the average discharge power of oxygen plasma for the decomposition of adsorbed VOC and gas flow rate during the adsorption period, respectively. t_{Oxy} and t_{Ads} indicate the period of oxygen plasma and the time of adsorption, respectively.

Optical emission was measured using a multi channel analyzer (Hamamatsu Photonics, C8808) and a UV lens (A960H). OES was measured without catalyst packing.

2.5. Chemical analysis

A Fourier transform infrared (FTIR) spectrometer (PerkinElmer, spectrum one), equipped with a gas cell of 6.4 m optical pathlength and a TGS detector, was used for quantitative gas analysis. To minimize a baseline fluctuation, which is unfavorable to the qualitative measurement, the space between the main body of the FTIR and the gas cell was purged with pure nitrogen. Gas measurements were done at 1 min intervals and two scans were averaged at a resolution of 1 cm^{-1}. The gas cell (0.75 L) was heated to 343 K to prevent any possible condensation during the measurement. FTIR analysis indicated that the decomposed benzene was mostly converted to CO_2 and CO, and small amount of formic acid (HCOOH) for certain conditions. Therefore, we simply calculated the carbon balance from the sum of CO, CO_2 and HCOOH. The CO_2 selectivity (S_{CO_2}), the carbon balance and the decomposition efficiency were obtained as follows:

$$S_{CO_2}(\%) = \frac{CO_2}{CO_2 + CO} \times 100 \quad (3)$$

$$\text{carbon balance}(\%) = \frac{CO + CO_2 + HCOOH}{n([VOC]_0 - [VOC])} \times 100 \quad (4)$$

$$\text{decomposition efficiency}(\%) = \frac{[VOC]_0 - [VOC]}{[VOC]_0} \times 100 \quad (5)$$

Here $[VOC]_0$ and n indicate inlet concentrations of VOC and the number of carbon atoms in them, respectively.

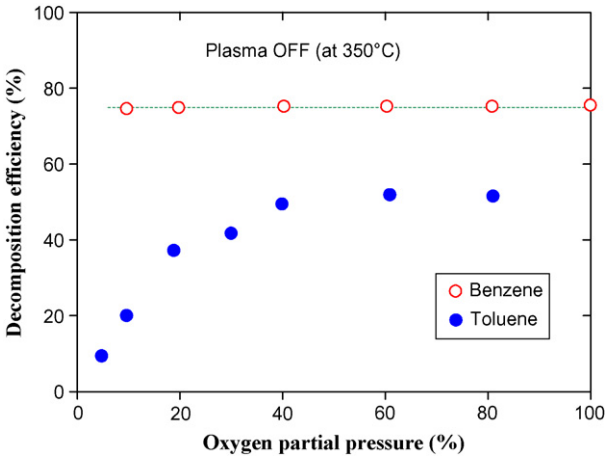

Fig. 3. The influence of oxygen partial pressure on the thermal catalysis of benzene and toluene over the 2.0 wt% Ag/TiO_2 catalyst. Space velocities for benzene and toluene were 22,000 h^{-1} and 33,000 h^{-1}, respectively.

3. Results and discussion

3.1. Effect of oxygen partial pressure on the conventional thermal catalysis and the plasma alone

3.1.1. Conventional thermal catalysis (without plasma)

Fig. 3 shows the influence of O_2 partial pressure on the conventional thermal catalysis of benzene and toluene over the 2.0% Ag/TiO_2 at 623 K. Thermal catalysis of benzene was completely independent of the O_2 partial pressure over the tested range. On the other hand, the decomposition efficiency of toluene increased with O_2 partial pressure up to 40%, and then leveled off toward higher O_2 partial pressure. Similar results were reported for the decomposition of toluene (~60 ppm) over V_2O_3-WO_3/TiO_2 catalyst, where the decomposition efficiency was independent of the initial O_2 concentration [27]. In the decomposition of dichlorobenzene (DCB, 600 ppm) over V_2O_3/TiO_2 catalyst, the oxidation rate of DCB depended on the O_2 partial pressure below 2%, but became independent at O_2 partial pressure larger than about 2% [28].

From the experimental data of thermal catalysis and the relevant literature information, it can be concluded that the highly O_2 partial pressure-dependent behavior of the PDC reactor is controlled by different mechanisms to the thermal catalysis.

3.1.2. Plasma alone process (without catalyst)

The role of oxygen in the electrical discharge plasma has been the subject of extensive studies both in chemistry and physics. The influences of oxygen on the plasma physics include photoionization [29], streamer property [30,31], electron attachment [32,33], transition of filamentary to glow discharge in dielectric-barrier discharge [34,35] etc. Fig. 4 shows the influence of O_2 partial pressure on the DBD decomposition (i.e. without catalysts) of (a) benzene and toluene, and (b) their selectivities of CO_2. The SIE of 305–310 J/L is believed to be high enough to avoid any influence from aerosol formation [15], and also to keep good carbon

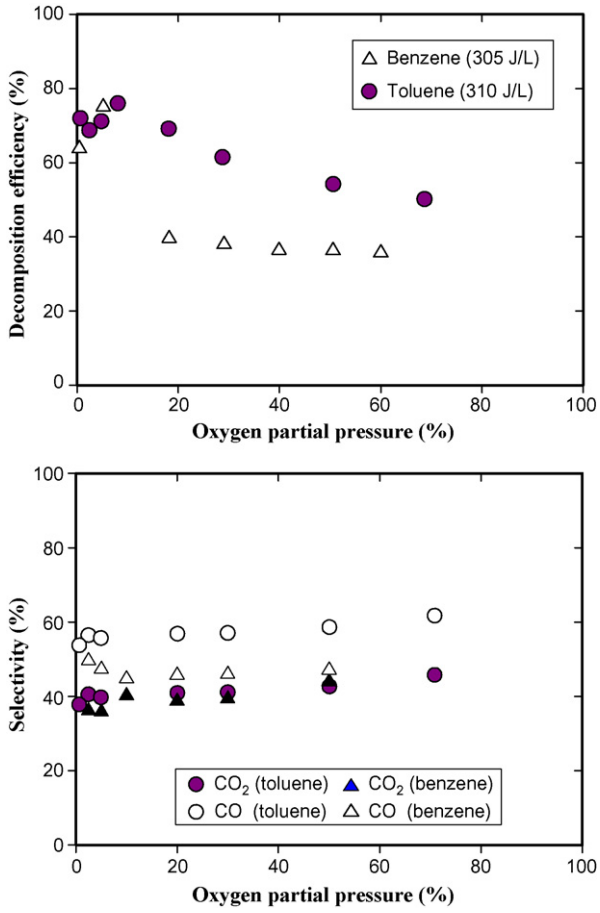

Fig. 4. The influence of oxygen partial pressure on the decomposition of benzene and toluene using DBD plasma reactor without any catalysts. Initial concentration was 200 ppm for both cases.

balance (sum of CO and CO_2 in this case). The O_2 partial pressure had negligible influence on the discharge current (i.e. SIE). The decomposition efficiencies of both benzene and toluene went through maximum at around 3–5% O_2, and then decreased drastically as the O_2 partial pressure further increased. The benzene decomposition was almost constant at O_2 partial pressure higher than 20%. In contrast to the decomposition efficiency, the selectivities of CO and CO_2 were much less influenced by the O_2 partial pressure even lower than 10% O_2. In both cases of benzene and toluene, the S_{CO} was higher than the S_{CO_2}. The O_2-dependent variations of VOC decomposition have been also reported by several researchers for the DBD plasma decomposition of chlorobenzene (maximum efficiency at 2.67% O_2) [36], C_2F_6 (5% O_2) [37], TCE (0.3% O_2) [38], toluene (5% O_2) [39]. Similar trends were observed in the decomposition of dichloromethane (CH_2Cl_2) using a $BaTiO_3$ packed-bed reactor (maximum efficiency at 2% O_2) [40], and conversion of 1-octene and 1-dodecene using a low-pressure plasma [41,42]. In addition to the decomposition efficiency, no O_2 dependence of S_{CO_2} was also reported for the decomposition of CH_3Br [43] and benzene [22,44] both using ferroelectric packed-bed reactors.

A possible reason for the higher VOC destruction at lower O_2 partial pressure is possibly due to the contribution of N radicals and excited N_2 molecules. The rate constants of the reactions with benzene suggest that the role of $N_2(A^3\Sigma_u^+)$ is more likely than that of N radical (no available data for toluene) [45]. $N_2(A^3\Sigma_u^+)$, the lowest electronically excited state of N_2, has a large excitation energy of 6.2 eV, which is greater than the bond energies of most molecules. The reaction R1 is even more faster than the O-benzene ($k = 1.6 \times 10^{-14}$ cm^3 molecule^{-1} s^{-1}) and O-toluene ($k = 7.9 \times 10^{-14}$ cm^3 molecule^{-1} s^{-1}) reactions at 300 K. The quenching of $N_2(A^3\Sigma_u^+)$ becomes significant as O_2 partial pressure increases [46], so its contribution to the decomposition of VOCs decreases. The increased O_2 partial pressure produces more O atoms by direct electron-impact dissociation and the collision dissociation by $N_2(A^3\Sigma_u^+)$, R4, as well.

$$N_2(A^3\Sigma_u^+) + \text{benzene} \rightarrow \text{products} \quad (k = 1.6 \times 10^{-10}\ \text{cm}^3\ \text{molecule}^{-1}\ \text{s}^{-1}) \tag{R1}$$

$$\text{N} + \text{benzene} \rightarrow \text{products} \quad (k < 10^{-15}\ \text{cm}^3\ \text{molecule}^{-1}\ \text{s}^{-1}) \tag{R2}$$

$$N_2(A^3\Sigma_u^+) + O_2 \rightarrow N_2 + O_2 \quad (k = 2.4 \pm 0.5 \times 10^{-12}\ \text{cm}^3\ \text{molecule}^{-1}\ \text{s}^{-1}) \tag{R3}$$

$$N_2(A^3\Sigma_u^+) + O_2 \rightarrow N_2 + 2O \quad (k = 2.5 \times 10^{-12}\ \text{cm}^3\ \text{molecule}^{-1}\ \text{s}^{-1}) \tag{R4}$$

The increased O_2 partial pressure also concurrently enhances the consumption of O atoms, which leads to the formation of O_3. Due to the small reaction rate of O_3 towards benzene and toluene in gas-phase, it does not contribute to the decomposition of benzene and toluene.

3.2. The oxygen partial pressure-dependence of different catalysts

3.2.1. TiO_2 catalyst

Fig. 5 shows the effect of O_2 partial pressure on the decomposition of benzene according to the type of metal catalysts and their loading amount. It should be noted that the SIE shown in the figure indicates the values at 20% O_2 because the discharge power slightly increased with O_2 even at a fixed voltage and frequency. As common trend, the decomposition efficiency of benzene linearly increased with O_2 partial pressures. The loading amount of Ag, from 0 wt% (TiO_2 alone) up to 2.0 wt%, gave rise to no prominent differences in the decomposition efficiency. However, the degree of enhancement lowered at 4.0 wt% Ag, which is believed due to the decrease of BET surface area. There were no differences between the Pt and Ag catalysts in terms of benzene decomposition. The influence of O_2 partial pressure on the CO_2 selectivity (Fig. 6) was less significant compared with those of decomposition efficiency (Fig. 5). In the case of TiO_2 alone, no enhancement was observed for the S_{CO_2} at O_2 partial pressure larger than 20%. In contrast to the decomposition efficiency, the larger the loading amount of Ag the higher the S_{CO_2} for a broad range of O_2 partial pressure. Although there is

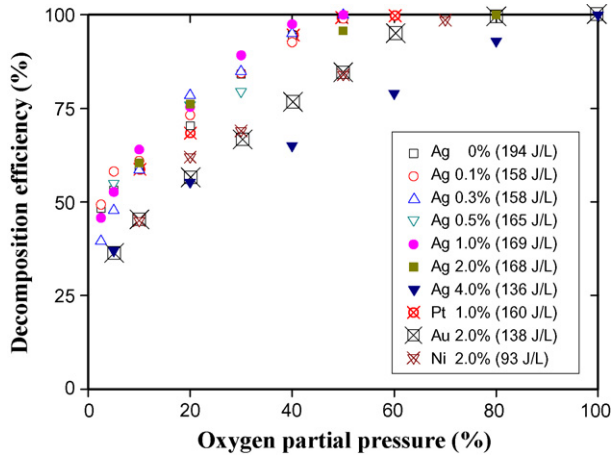

Fig. 5. Oxygen partial pressure-dependent behavior of the PDC reactor packed with TiO_2 with different metal catalysts. Specific input energies in the figure indicate the values at 20% oxygen.

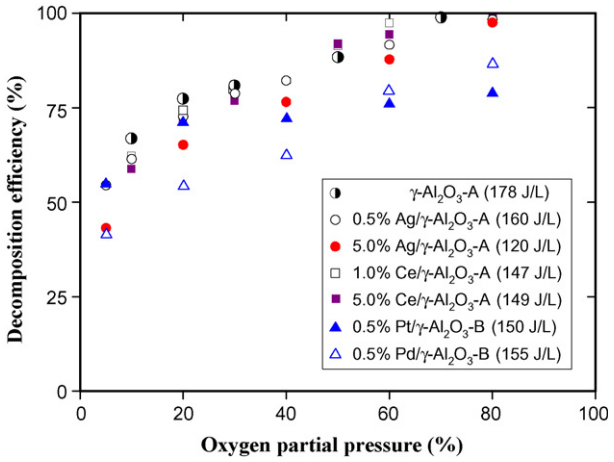

Fig. 7. Oxygen partial pressure-dependent behavior of the PDC reactor packed with γ-Al_2O_3 with different metal catalysts.

a difference in the loading amount, Au showed the highest S_{CO_2} and followed by Pt, Ag (in its loading amount) and Ni.

3.2.2. γ-Al_2O_3 catalyst

Fig. 7 shows the effect of O_2 partial pressure on benzene decomposition with two different γ-alumina catalysts. For both γ-Al_2O_3-A and γ-Al_2O_3-B, the higher the O_2 partial pressure the better the decomposition efficiency. As similar to the TiO_2 case, the enhancement of benzene decomposition was also observed with the bare γ-Al_2O_3-A. The supporting of Ag and Ce catalysts and their supporting amount did not change the degree of benzene decomposition. The Pd/γ-Al_2O_3-B also showed similar trend to the γ-Al_2O_3-A cases. The Pt/γ-Al_2O_3-B catalyst showed the least sensitivity to the change of O_2 partial pressure.

Fig. 8 shows the influence of O_2 partial pressure on the S_{CO_2}. The Pd and the Pt supported γ-Al_2O_3-B catalysts were more effective than the γ-Al_2O_3-A catalysts in terms of the S_{CO_2}, especially at lower O_2 partial pressure. As in the case of the Pt/TiO_2, the increase of O_2 partial pressure did not enhance the S_{CO_2} with the Pt/γ-Al_2O_3-B catalyst. The influence of O_2 partial pressure on the S_{CO_2} was more significant for the γ-Al_2O_3-A catalysts than the γ-Al_2O_3-B catalysts. In contrast to the TiO_2 catalyst, the amount of Ag supported on the γ-Al_2O_3-A has no influence on the S_{CO_2}.

3.2.3. Zeolites

Fig. 9 shows the O_2 partial pressure-dependence of zeolites in the benzene decomposition. The ferrierite showed the least enhancement of decomposition efficiency according to the increase of O_2 partial pressure. In the case of H-Y zeolite, the decomposition efficiency of benzene linearly increased with O_2 partial pressure, and reached 100% at about 80% oxygen. The supported 2.0 wt% Ag catalyst on the H-Y did not affect the benzene decomposition. Because of the large adsorption capacity of the MS-13X, equilibrium data could not obtain for the. The data points of the MS-13X are the outlet CO_x concentration, and the error bars stand for the unmeasured portion by adsorption. The MS-13X also exhibited positive enhancement of the benzene decomposition as the O_2 partial

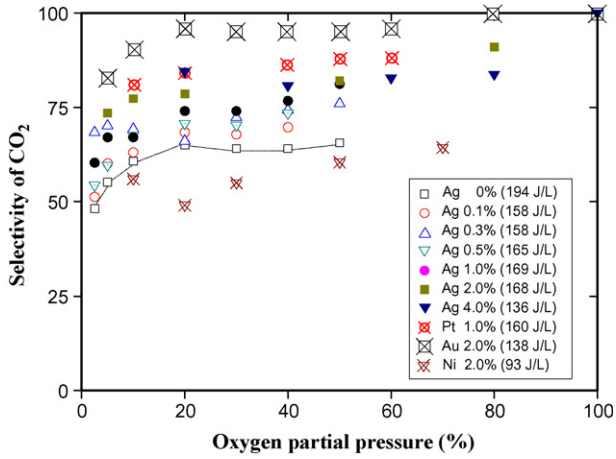

Fig. 6. The effect of oxygen partial pressure on the selectivity of CO_2 in the PDC reactor packed with TiO_2.

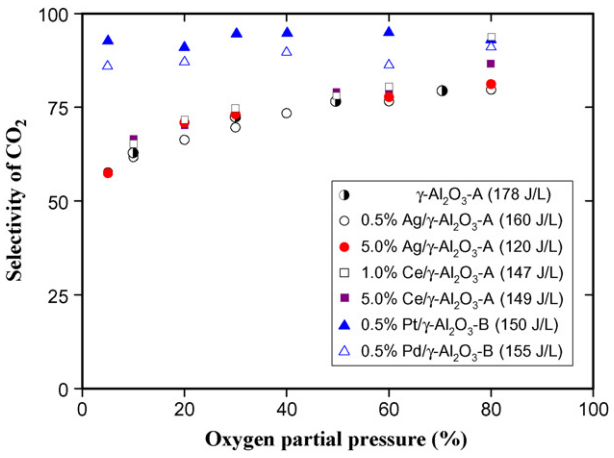

Fig. 8. The effect of oxygen partial pressure on the selectivity of CO_2 in the PDC reactor packed with γ-Al_2O_3.

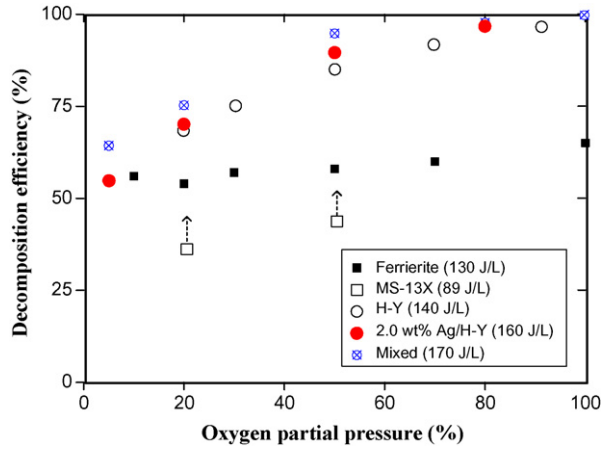

Fig. 9. Oxygen partial pressure-dependent behavior of the PDC reactor packed with various zeolites.

pressure increased. The mechanical mixing of the Pt/γ-Al_2O_3-B catalyst (25%) with the 2% Ag/H-Y (75%) slightly increased the decomposition efficiency of benzene.

Fig. 10 shows the influence of O_2 partial pressure on the S_{CO_2}. Despite the ferrierite showed the least degree of enhancement in the benzene decomposition, the enhancement of S_{CO_2} with O_2 partial pressure was most prominent with the ferrierite. The presence of Ag on the H-Y zeolite did not affect the S_{CO_2} at all. The S_{CO_2} of the 2% Ag/H-Y was enhanced by the mechanical mixing with the Pt/γ-Al_2O_3-B. This observation suggests that the combination of good adsorbent with proper catalysts can be promising for the optimization of VOCs decomposition using the cycled system.

3.3. Carbon balance

Fig. 11 summarizes the influence of O_2 partial pressure on the carbon balance for the tested catalysts. Except for the Ni/TiO_2 catalyst, TiO_2 catalysts exhibited good carbon balances (95–106%) regardless of the type of metal catalysts and their supporting amount. The good carbon balance with Ag/TiO_2

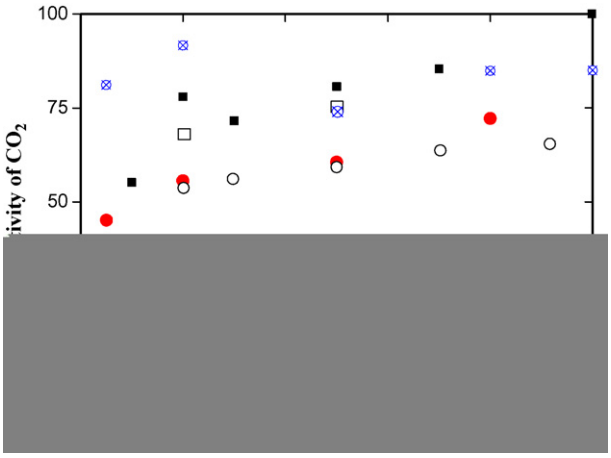

Fig. 10. The effect of oxygen partial pressure on the selectivity of CO_2 in the PDC reactor packed with various zeolites.

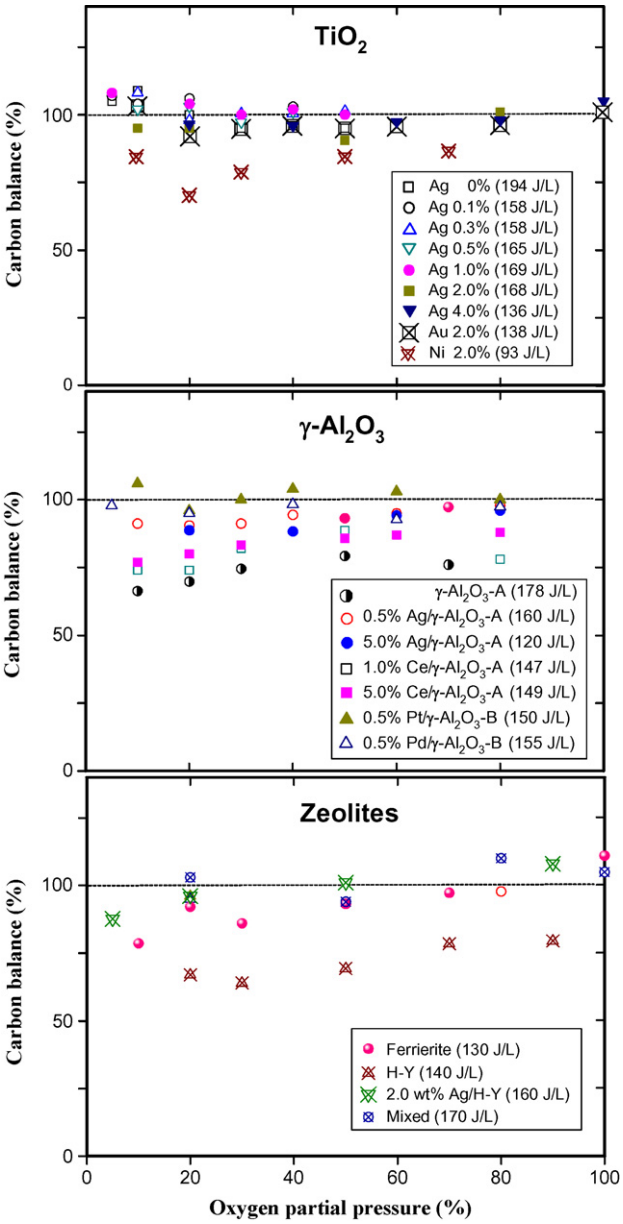

Fig. 11. Carbon balance.

catalysts was also demonstrated by the long-term operation over 150 h and the relevant FE-SEM images [17]. The effect of the metal catalyst was more prominent with the γ-Al_2O_3-A and H-Y zeolite than the TiO_2. The bare γ-Al_2O_3-A had poor carbon balances at 66–88%. The supported Ce and Ag catalysts enhanced the carbon balance. Pt and Pd catalysts supported on the γ-Al_2O_3-B were very effective to obtain good carbon balance. The supporting of Ag on the H-Y had no influence both on the benzene decomposition and the S_{CO_2}. Nevertheless, the largest enhancement (about 30%) in carbon balance by supporting 2.0 wt% Ag catalyst was observed with the H-Y zeolite. As indicated by the temperature-programmed desorption and oxidation (TPD and TPD) [47,48], the poor carbon balance with the bare γ-Al_2O_3-A and bare H-Y may be due to the formation of carbonaceous products, HCOOH and the adsorption of CO_2 as well. The mixed catalyst was also found to be effective in enhancing carbon balance.

3.4. Formation of nitrogen oxides

Nonthermal plasma in air-like mixtures produces N_xO_y compounds. The type of N_xO_y strongly depends on the operating conditions such as reactor type, SIE range, temperature, and humidity etc. In the case of the PDC reactors, two important N_xO_y species were NO_2 and N_2O. NO was not observed in the presence of O_3, but it can be observed only at high SIE range. Fig. 12 shows the formation of NO_2 and N_2O in the flow-type PDC system as a function of the oxygen partial pressure in the gas stream. The formation of NO_2 changed drastically with the oxygen partial pressure. The maximum formation was observed at about 10–20% oxygen, and then decreased with further increase of oxygen. Similar trends have been also observed in the pulsed arc discharge [49] and pulsed discharge [50] in O_2–N_2 mixtures. The formation of NO_x reached maximum at around 30–40% oxygen. On the other hand, the N_2O concentration was quite sensitive to the oxygen partial pressure below 10%, and leveled off at higher oxygen partial pressure. The data shown in Fig. 12 clearly indicate that the increase of oxygen partial pressure can reduce the formation of nitrogen oxide, but not completely. From a practical standpoint, the need for the rapid regeneration of adsorbents may render the plasma energy to be maintained at high level.

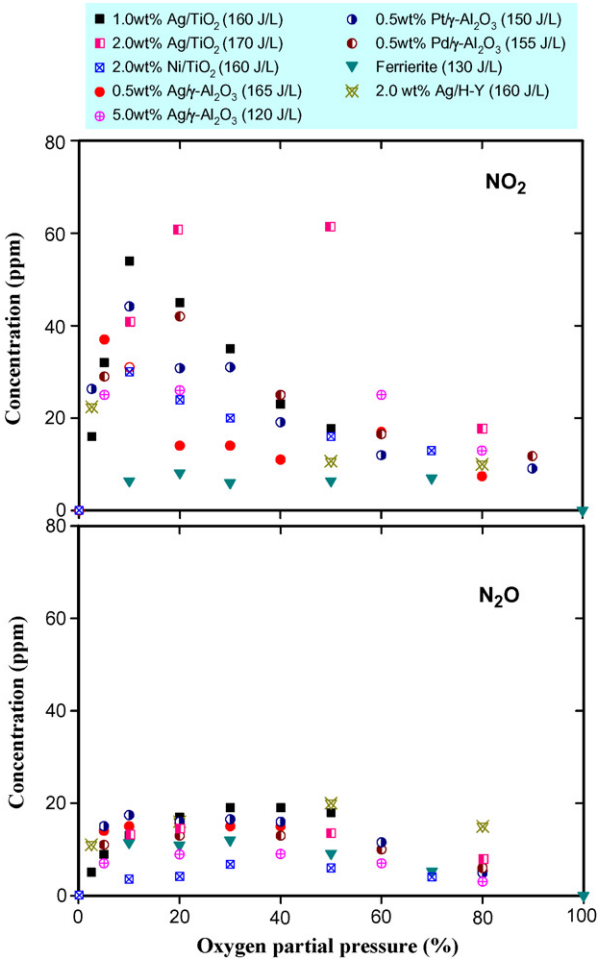

Fig. 12. The effect of oxygen partial pressure on the formation of NO_2 and N_2O.

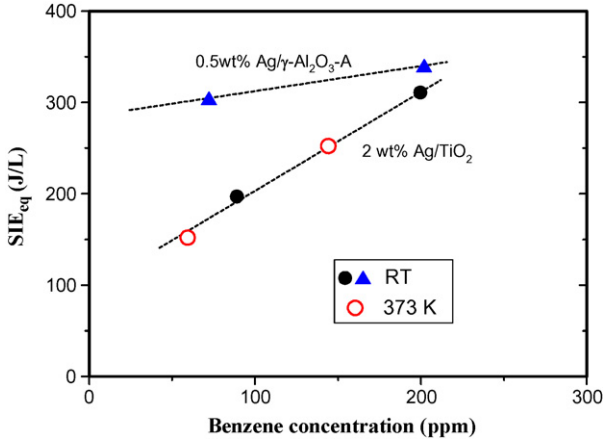

Fig. 13. Equivalent specific input energy for the decomposition of adsorbed benzene.

Therefore, oxygen plasma will be necessary for the complete suppression of N_xO_y formation.

3.5. The effects of concentration and temperature on the VOC decomposition using the cycled operation

Fig. 13 shows the SIE_{eq} for the complete decomposition of benzene using the cycled system. The SIE_{eq} for the complete oxidation of adsorbed benzene linearly depended on its initial concentration. The higher the initial concentration, the larger the SIE_{eq} for the complete oxidation of adsorbed benzene. This result can be explained by the zeroth-order kinetics of the PDC system, where the amount of decomposed VOCs is only determined by SIE rather than its concentration [16,17]. The required SIE_{eq} obtained at room temperature and 373 K fell on single line. In the flow-type test (see Fig. 5), 200 ppmv of benzene was completely decomposed with about 170 J/L, while SIE_{eq} of 300 J/L for the cycled operation. The high SIE_{eq} may ascribe to the additional PDC reactor used in the regeneration mode. Therefore it will be possible to further decrease the SIE_{eq} by optimizing the system configuration and the use of proper adsorbent/catalyst. The Ag/γ-Al_2O_3-A catalyst consumed more energy than the Ag/TiO_2 catalyst due to the small enhancement factor (see Section 4).

The oxygen-PDC completely oxidized the adsorbed VOCs to CO_2, which is impossible with the conventional plasma alone process or the flow-type PDC system. A further advantage of the cycled system is its adaptability to the broad range changes in the flow rate or the VOCs concentration, which are usually difficult to treat using the flow-type plasma reactors. In addition to the high energy efficiency and the CO_2 selectivity, this oxygen PDC system does not produce nitrogen oxides (N_xO_y) at all.

4. Discussion

4.1. Mapping of catalyst potentials for the cycled system

Fig. 14 summarizes the potential of the tested catalysts for the cycled system in terms of adsorption capability and the

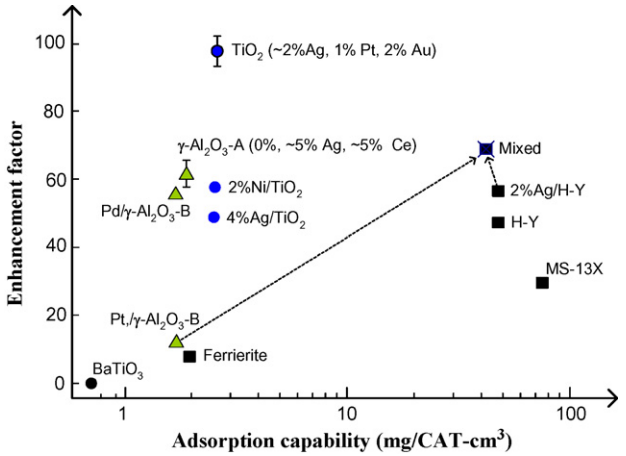

Fig. 14. Mapping of various catalysts in terms of adsorption capability and enhancement factor. The adsorption capability is based on the benzene experiment at 373 K.

enhancement factor. The enhancement factor is defined as the ratio of decomposition efficiency with respect to the oxygen partial pressure at the same SIE.

$$\text{Enhancement factor} = \frac{\eta_{\text{Oxygen}} - \eta_{\text{Air}}}{[\text{O}_2]_{\text{Oxygen}} - [\text{O}_2]_{\text{Air}}} \times 100 \quad (6)$$

where η_{Oxygen} and η_{Air} indicate the decomposition efficiency of VOCs in air and oxygen, respectively. The physical meaning of the enhancement factor is the slope of decomposition efficiency with respect to O_2 partial pressure (see Figs. 5, 7 and 9) at a given SIE. In the case that the decomposition efficiency reached 100% at O_2 partial pressure below 100% O_2, $[O_2]_i$, the enhancement factor was calculated from the slope of decomposition efficiency between $[O_2]_{\text{Air}}$ and $[O_2]_i$. The SIE range (100–200 J/L) used was selected by considering the carbon balance and the degree of decomposition efficiency. When the SIE is smaller than about 100 J/L, carbon balance is not satisfactory [17,18]. On the other hand, the removal efficiency becomes high (more than 90%) under the SIE larger than 200 J/L even at air-like mixture (i.e. 20% oxygen). Therefore it is difficult to find the difference in the decomposition efficiency by varying the oxygen content. It should be noted that the enhancement factor could also be influenced by SIE. But this was not included in the current evaluation, and will be reported elsewhere.

One important finding in this work is that all the tested materials exhibited positive values in enhancement factor. In contrast, enhance factors with the DBD plasma alone were found to be negative (−11 for benzene, −40 for toluene). The TiO_2 catalysts showed the highest enhancement factor at about 100. However, the adsorption capability of TiO_2 being too small for the cycled system. For zeolites, the highest enhancement factor was obtained with the 2 wt% Ag/H-Y and followed by the H-Y, the MS-13X, and the ferrierite. The ferrierite was good in terms of S_{CO_2}, but it had low adsorption capability and the small enhancement factor as well. The mechanical mixing of 2.0 wt% Ag/H-Y with Pt/γ-Al_2O_3 was found to be effective in enhancing the enhancement factor and the CO_2 selectivity.

4.2. Plausible mechanism

Many of recent publications reported the synergetic effect in the plasma–catalyst decomposition of VOCs even at low temperatures, where the normal thermal catalysis does not occur. Although the detailed mechanism is still unclear at this stage, the synergetic effect can be explained by the involvement of catalyst surface activated by plasma. Some hypotheses have been proposed for the possible mechanism in plasma–catalyst systems. These include ozone, UV, local heating, changes in work function, activation of lattice oxygen, plasma-induced adsorption/desorption, generation of electron–hole pairs and their subsequent chemical reactions, direct interaction of gas-phase radicals with the catalyst surface and the adsorbed molecules etc. The plasma-induced desorption and the decomposition of adsorbed molecules can clean the active sites of catalyst, which also lead to a high performance. The interaction between the adsorbed molecule and solid surface could affect the catalytic activity. When a molecule having bond energy of E_b is adsorbed on a surface, E_b will be weakened according to the degree of adsorption energy (E_{ad}), which is determined by the type of adsorption (i.e. physisorption or chemisorption) [51]. Therefore, the barrier for the chemical reaction may be lowered to amount proportional to E_b–E_{ad}, resulting in the enhancement of chemical reactivity.

Several experimental observations strongly suggest that the contribution of UV seems to be less important in the PDC system. First, the space velocities in PDC system (~80,000 h^{-1}) is 2–3 orders of magnitude larger than those in the UV-photocatalyst (normally less than several hundreds h^{-1}) [52,53]. Second, UV activation mechanism is less plausible in γ-Al_2O_3 cases due to its large band gap energy of about 7.2 eV (equivalent photon energy of 172 nm) [54], which is far above the photon energy of atmospheric pressure O_2 plasma (normally 400–900 nm). The intensity of UV emission also decreases as O_2 concentration increases [55]. Nevertheless, both the decomposition efficiency and the S_{CO_2} were the highest in oxygen plasma for all the tested catalysts in this study. Previous study comparing the benzene decomposition under different dilution gases (N_2, Ar) also confirmed the negligible contribution of UV emission even for the TiO_2 catalyst [16]. Sano et al. studied the plasma–catalyst decomposition of CH_3CHO and found that the UV contribution was less than 0.2% [56]. Therefore, the contribution of UV light in the plasma-driven catalysis was excluded from the mechanism.

Fig. 15 summarizes plausible mechanism for the plasma-driven catalysis of VOCs based on the experimental data in this study together with those in literature. The solid lines are proposed based on the experimental observations. The dotted lines indicate the expected pathways but lack in the supporting experimental evidence at this stage. Two important models explaining the catalytic reactions are Langmuir–Hinshelwood (L–H) model and Eley–Rideal (E–R) model. In the L–H model, both of the reactants need to be absorbed on the surface, and

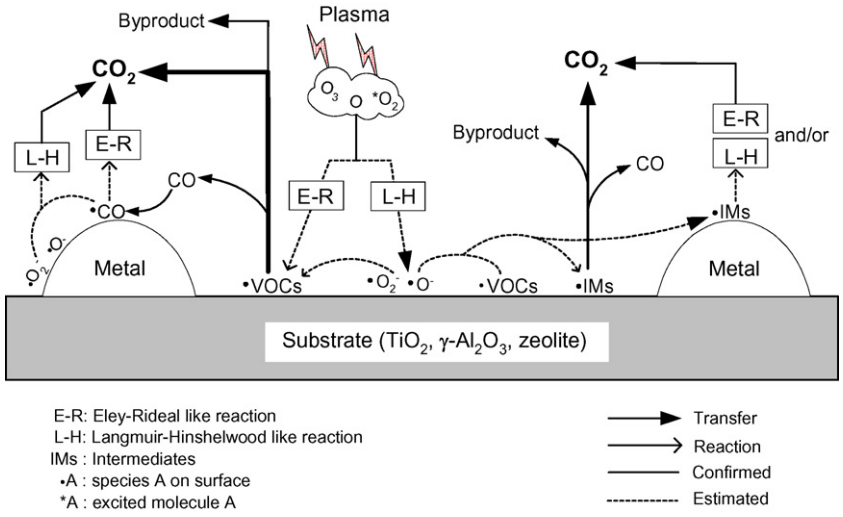

Fig. 15. Plausible mechanism for the plasma-driven catalysis of VOCs.

followed by migration to active site. In the E–R model, only one reactant is adsorbed on the surface and the other exists in gas-phase. In conventional thermal catalysis of VOCs (i.e. plasma off), dissociative chemisorption of O_2 onto metal oxides (such as TiO_2, γ-Al_2O_3, ZrO_2 etc.) produces reactive surface species (such as O_2^- and O^-), which lead to the oxidative removal of pollutants.

$$O_{2(g)} + CAT* \rightarrow O_{2(s)}{}^- + CAT \quad (R5)$$

$$O_{2(s)}{}^- + e \rightarrow O_{(s)}{}^- + O^-{}_{(s)} \quad (R6)$$

Here the subscripts (g) and (s) indicate the species in gas-phase and surface, respectively. This dissociative chemisorption of O_2 cannot explain the strong O_2 partial pressure-dependence of the PDC system, because this trend was not observed in the thermal catalysis (see Fig. 3). When a plasma is applied to the PDC reactor, reactive surface oxygen species can be also generated from the lattice oxygen [57] and direct interaction with $O_{3(g)}$ [13,14], or $O_{(g)}$ radicals as well [58].

$$\text{Lattice-}O_{(s)} + \text{plasma} \rightarrow O_{(s)}{}^- + CAT \quad (R7)$$

$$O_{3(g)} + CAT* \rightarrow O_{(s)}{}^- + O_{2(s)} + CAT \quad (R8)$$

$$O_{(g)} + CAT* \rightarrow O_{(s)}{}^- + CAT \quad (R9)$$

The adsorbed surface species can also migrate from one site to the other and eventually disappear via recombination and chemical reactions. The NTP can also promote desorption of reaction products, which is helpful to keep the catalytic activity. Both the current study and our previous work [18] strongly suggested that the removal of VOCs proceeds mainly on the surface of the main catalysts (TiO_2, γ-Al_2O_3, zeolites) rather than on the supported metal catalysts. It should be also noted that the PDC reactor (even with the bare catalysts without supported metals) always exhibited higher S_{CO_2} (50–99%, see Figs. 6, 8 and 10) than that of the DBD alone (ca. 40%). However, it is difficult to further oxidize CO using the bare catalysts without supported metals. These experimental data supported that the large enhancement in S_{CO_2} can be attributed to the surface reactions on main catalysts (TiO_2, γ-Al_2O_3, zeolites), and the supporting metal catalyst lead to further oxidation of gas-phase CO. In most catalysts tested, the effect of O_2 partial pressure was more prominent in the decomposition efficiency than that of the S_{CO_2}. For the bare TiO_2 and γ-Al_2O_3, however, O_2 partial pressure showed little or no influence on the S_{CO_2}. The supported metal catalysts also led to good carbon balance (Fig. 11) even at lower SIE range [18]. HCOOH was found to be an important intermediate for the CO_2 formation in the decomposition of aromatic VOCs [17].

The strong dependence of VOC decomposition on the O_2 partial pressure can be explained by the increased formation of reactive oxygen species and the subsequent interactions with catalysts. Fig. 16 shows the O atom intensity at 777 nm line as a function of O_2 partial pressure. The optical intensity of O atom showed linear dependence on the O_2 partial pressure. A linear dependence of O density on O_2 concentration was also reported microwave plasma [59] and pulsed rf plasma [60] both in low-pressure (0.1–10 Torr). These OES data correlate closely with

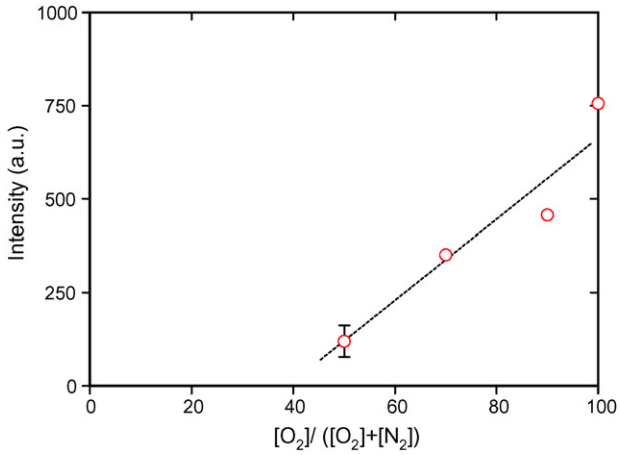

Fig. 16. Relative intensity of O atom at 777 nm line as a function of O_2 partial pressure. This OES was measured in the absence of catalysts. Applied voltage and the frequency were 24 kV_{pk-pk} and 300 Hz, respectively.

the O_2-dependent decomposition efficiency of VOC. However, gas-phase homogeneous reactions are too slow to make significant contribution to the decomposition of VOCs. For example, the rate constants for the reaction of benzene with $O(^3P)$ and O_3 are 1.76×10^{-14} cm^3 molecule^{-1} s^{-1} and 1.72×10^{-22} cm^3 molecule^{-1} s^{-1} at 298 K, respectively.

$$\text{Benzene} + O(^3P) \rightarrow \text{product} \quad \text{(R10)}$$

$$\text{Benzene} + O_3 \rightarrow \text{product} \quad \text{(R11)}$$

Therefore, the interaction of reactive oxygen species and catalysts is expected to play an important role in the synergetic effect. It will be challenging subject to study the behavior of the reactive oxygen species on the catalyst surface.

There have been some relevant reports indicating the importance of E–R like reaction in single-stage plasma–catalyst system. For example, atomic oxygen enhanced the CO oxidation over Au catalyst in a CO_2 laser [61]. Petersson et al. studied the O_3 enhanced CO oxidation over a Pt/γ-Al_2O_3 catalyst (i.e. two-stage process) [62], and observed an E–R like reaction, in which adsorbed CO on Pt reacted with gas-phase O_3 molecules. We have observed the enhancement of CO oxidation , which can be explained better by the E–R model than the L–H model in the CO oxidation on the gold nanoparticle catalyst supported on TiO_2 [63]. *In situ* plasma greatly enhanced the oxidation of gas-phase CO over the used Au/TiO_2, which has completely lost its catalytic activity. However, it is still premature to make any conclusion on which model is more likely to occur in the PDC system. For the better understanding of the plasma–catalyst interaction, it will be necessary to collect more information regarding what are key reactive species, where they are adsorbed, and where and how the species react with adsorbed VOCs.

5. Conclusions

In this study, the potentials of various catalysts for the cycled system were evaluated. A new parameter of enhancement factor was introduced to determine the oxygen partial pressure-dependent behavior of the tested catalysts. The main findings of this work can be summarized as follows.

(1) Conventional thermal catalysis of benzene was independent of the oxygen partial pressure. In the case of toluene, decomposition efficiency increased with O_2 partial pressure up to 40% and then leveled off at higher O_2 partial pressure.
(2) In the case of the DBD plasma reactor, the increase of O_2 partial pressure above 20% had little or minor influence on the decomposition of benzene and toluene.
(3) In the case of PDC reactor, the increase of O_2 partial pressure enhanced both the decomposition efficiency of benzene and the S_{CO_2} regardless of the type of catalysts (TiO_2, γ-Al_2O_3, zeolites). The degree of O_2-dependent variation was more significant with the decomposition efficiency than the S_{CO_2}. Among tested materials in this work, TiO_2 catalysts showed the largest enhancement factor of about 100.
(4) The mechanical mixing of the Pt/γ-Al_2O_3-B and Ag/H-Y was found to be effective in enhancing the S_{CO_2} without changing the other performance.
(5) At fixed SIE, the formation of NO_2 went through maximum at about 20%, and decreased with further increase of O_2. On the other hand, the formation of N_2O was quite constant for O_2 partial pressure up to about 50% and decreased at higher O_2 partial pressure. These data clearly show that the regeneration mode in the cycled system must be done at pure oxygen for the complete suppression of the N_xO_y formation.
(6) The supported metal catalysts played important roles in enhancing both the S_{CO_2} and the carbon balance. The initial step of VOCs decomposition proceeded mainly on the surface of the main catalysts (TiO_2, γ-Al_2O_3, zeolites). Based on the experimental results and the some relevant information in literature, a mechanism of plasma-driven catalysis of VOCs was suggested.

In future work, it will be of interest to see which mechanism has more contribution and, what chemical species play dominant role in the decomposition of VOCs. Although well-designed instruments specialized for the *in situ* measurement of PDC system is not available yet, direct measurement of reactive chemical species and the reaction intermediates will be challenging research object in the future.

Acknowledgements

The authors appreciate Dr. M. Date and Dr. S. Tsubota for the preparation of the Au/TiO_2 catalyst by deposition–precipitation method. Parts of this work was supported by Ministry of Education, Culture, Sports, Science and Technology (MEXT); Grand-in-Aid for Young Scientist (A) (16681007).

References

[1] A. Mizuno, J.S. Clements, R.H. Davis, IEEE Trans. Ind. Appl. 22 (1986) 516.
[2] T. Yamamoto, K. Ramanathan, P.L. Lawless, D.S. Ensor, J.R. Newsome, N. Plaks, G.H. Ramsey, IEEE Trans. Ind. Appl. 28 (1992) 528.
[3] G. Dinelli, M. Rea, J. Electrostat. 25 (1990) 23.
[4] H.H. Kim, Plasma Process. Polym. 1 (2004) 91.
[5] A. Ogata, D. Ito, K. Mizuno, S. Kushiyama, T. Yamamoto, IEEE Trans. Ind. Appl. 37 (2001) 959.
[6] Y.H. Song, S.J. Kim, K.I. Choi, T. Yamamoto, J. Electrostat. 55 (2002) 189.
[7] F. Holzer, U. Roland, F.-D. Kopinke, Appl. Catal. B: Environ. 38 (2002) 163.
[8] S. Masuda, S. Hosokawa, X. Tu, M. Tsutsumi, T. Ohtani, T. Tsukahara, N. Matsuda, IEEE Trans. Ind. Appl. 29 (1993) 774.
[9] A. Gervasini, V. Ragaini, Catal. Today 60 (2000) 129.
[10] H. Einaga, T. Ibusuki, S. Futamura, IEEE Trans. Ind. Appl. 37 (2001) 1476.
[11] T. Hammer, Plasma Sources Sci. Technol. 11 (2002) 1.
[12] C. Reed, Y. Xi, S.T. Oyama, J. Catal. 235 (2005) 378.
[13] A. Naydenov, D. Mehandjiev, Appl. Catal. A: Gen. 97 (1993) 17.
[14] P. Konova, M. Stoyanova, A. Naydenov, S. Christoskova, D. Mehandjiev, Appl. Catal. A: Gen. 298 (2006) 109.
[15] H.H. Kim, H. Kobara, A. Ogata, S. Futamura, IEEE Trans. Ind. Appl. 41 (2005) 206.

[16] H.H. Kim, S.M. Oh, A. Ogata, S. Futamura, Appl. Catal. B: Environ. 56 (2005) 213.
[17] H.H. Kim, A. Ogata, S. Futamura, J. Phys. D: Appl. Phys. 38 (2005) 1292.
[18] H.H. Kim, A. Ogata, S. Futamura, IEEE Trans. Plasma Sci. 34 (2006) 984.
[19] A. Ogata, K. Miyamae, K. Mizuno, S. Kushiyama, T. Yamamoto, Plasma Chem. Plasma Proc. 22 (2002) 537.
[20] A. Rousseau, A. Dantier, L. Gatilova, Y. Ionikh, J. Ropcke, Y. Tolmachev, Plasma Sources Sci. Technol. 14 (2005) 70.
[21] T. Yamamoto, J. Hazard. Mater. B67 (1999) 165.
[22] H.H. Kim, S.M. Oh, A. Ogata, S. Futamura, J. Adv. Oxid. Technol. 8 (2005) 226.
[23] M. Haruta, S. Tsubota, T. Kobayashi, H. Kageyama, M.H. Genet, J. Catal. 144 (1993) 175.
[24] M. Haruta, N. Yamada, T. Kobayashi, S. Iijima, J. Catal. 115 (1989) 301.
[25] M. Daté, Y. Ichihashi, T. Yamashita, A. Chiorino, F. Boccuzzi, M. Haruta, Catal. Today 72 (2002) 89.
[26] H.J. White, J. Air Pollut. Control Assoc. 27 (1977) 308.
[27] K. Everaert, J. Baeyens, J. Hazard. Mater. B109 (2004) 113.
[28] S. Krishnamoorthy, J.P. Baker, M.D. Amiridis, Catal. Today 40 (1998) 39.
[29] G.W. Penney, G.T. Hummert, J. Appl. Phys. 41 (1970) 572.
[30] W.J. Yi, P.F. Williams, J. Phys. D: Appl. Phys. 35 (2002) 205.
[31] N.L. Aleksandrov, E.M. Bazelyan, G.A. Novitskii, J. Phys. D: Appl. Phys. 34 (2001) 1374.
[32] J.S. Clements, R.E. Williams, IEEE Trans. Ind. Appl. 31 (1995) 778.
[33] B.M. Penetrante, M.C. Hsiao, J.N. Bardsley, B.T. Merritt, G.E. Vogtlin, A. Kuthi, C.P. Burkhart, J.R. Bayless, Plasma Sources Sci. Technol. 6 (1997) 251.
[34] K.V. Kozlov, R. Brandenburg, H.E. Wagner, A.M. Morozov, P. Michel, J. Phys. D: Appl. Phys. 38 (2005) 518.
[35] R. Brandenburg, H.E. Wagner, A.M. Morozov, K.V. Kozlov, J. Phys. D: Appl. Phys. 38 (2005) 1649.
[36] H.R. Snyder, G.K. Anderson, IEEE Trans. Plasma Sci. 26 (1998) 1695.
[37] M.B. Chang, S.J. Yu, Environ. Sci. Technol. 35 (2001) 1587.
[38] Z. Falkenstein, J. Appl. Phys. 85 (1999) 525.
[39] Y.F. Guo, D.Q. Ye, K.F. Chen, J.C. He, W.L. Chen, J. Mol. Catal. A: Chem. 245 (2005) 93.
[40] C. Fitzsimmons, F. Ismail, J.C. Whitehead, J.J. Wilman, J. Phys. Chem. A 104 (2000) 6032.
[41] P. Patino, A. Mejia, P. Rodriguez, B. Mendez, Fuel 82 (2003) 1613.
[42] G. Gambus, P. Patino, B. Mendez, A. Sifontes, J. Navea, P. Martin, P. Taylor, Energy Fuel 15 (2001) 881.
[43] S. Futamura, Z. Zhang, T. Yamamoto, IEEE Trans. Ind. Appl. 35 (1999) 760.
[44] A. Ogata, N. Shintani, K. Mizuno, S. Kushiyama, T. Yamamoto, IEEE Trans. Ind. Appl. 35 (1999) 753.
[45] J.T. Herron, J. Phys. Chem. Ref. Data 28 (1999) 1453.
[46] M.F. Golde, Int. J Chem. Kinet. 20 (1988) 75.
[47] A. Ogata, H. Einaga, H. Kabashima, S. Futamura, S. Kushiyama, H.H. Kim, Appl. Catal. B: Environ. 46 (2003) 87.
[48] S.M. Oh, H.H. Kim, H. Einaga, A. Ogata, S. Futamura, D.W. Park, Thin Solid Films 506–507 (2006) 418.
[49] T. Namihira, S. Tsukamoto, D. Wang, S. Katsuki, R. Hackam, K. Okamoto, H. Akiyama, IEEE Trans. Plasma Sci. 28 (2000) 109.
[50] E. Franzblau, J. Geophys. Res. 96 (1991) 22337.
[51] D.E. Rapakoulias, S. Cavadias, D. Mataras, High Temp. Chem. Process. 2 (1993) 231.
[52] W. Wang, L. Chiang, Y. Ku, J. Hazard. Mater. B101 (2003) 133.
[53] Z. Pengyi, L. Fuyan, Y. Gang, C. Qing, Z. Wanpeng, J. Photochem. Photobiol. A: Chem. 156 (2003) 189.
[54] R.H. French, J. Am. Chem. Soc. 73 (1990) 477.
[55] N. Philip, B. Saoudi, M.C. Crevier, M. Moisan, J. Barbeau, J. Pelletier, IEEE Trans. Plasma Sci. 30 (2002) 1429.
[56] T. Sano, N. Negishi, E. Sakai, S. Matsuzawa, J. Mol. Catal. A: Chem. (2006) 235.
[57] A. Ogata, H.H. Kim, S. Futamura, S. Kushiyama, K. Mizuno, Appl. Catal. B: Environ. 53 (2004) 175.
[58] U. Roland, F. Holzer, F.-D. Kopinke, Catal. Today 73 (2002) 315.
[59] M.K. Boudam, B. Saoudi, M. Moisan, A. Ricard, J. Phys. D: Appl. Phys. 40 (2007) 1694.
[60] G. Dilecce, S.D. Benedictis, Plasma Sources Sci. Technol. 8 (1999) 266.
[61] J.A. Macken, S.K. Yagnik, M.A. Samis, IEEE J. Quantum Electron. 25 (1989) 1695.
[62] M. Petersson, D. Jonsson, H. Persson, N. Cruise, B. Andersson, J. Catal. 238 (2006) 321.
[63] H.H. Kim, S. Tsubota, M. Daté, A. Ogata, S. Futamura, Appl. Catal. A: Gen. 329 (2007) 93.